J. Fluid Mech. (1991), *vol.* 231, *pp.* 575–598
Printed in Great Britain

The stability of filamentary vorticity in two-dimensional geophysical vortex-dynamics models

By D. W. WAUGH AND D. G. DRITSCHEL
Department of Applied Mathematics and Theoretical Physics, University of Cambridge, Silver Street, Cambridge CB3 9EW, UK

(Received 7 December 1990)

The linear stability of filaments or strips of 'potential' vorticity in a background shear flow is investigated for a class of two-dimensional, inviscid, non-divergent models having a linear inversion relation between stream function and potential vorticity. In general, the potential vorticity is not simply the Laplacian of the stream function – the case which has received the greatest attention historically. More general inversion relationships between stream function and potential vorticity are geophysically motivated and give an impression of how certain classic results, such as the stability of strips of vorticity, hold under more general circumstances.

In all models, a strip of potential vorticity is unstable in the absence of a background shear flow. Imposing a shear flow that reverses the total shear across the strip, however, brings about stability, independent of the Green-function inversion operator that links the stream function to the potential vorticity. But, if the Green-function inversion operator has a sufficiently short interaction range, the strip can also be stabilized by shear having the same sense as the shear of the strip. Such stabilization by 'co-operative' shear does not occur when the inversion operator is the inverse Laplacian. Nonlinear calculations presented show that there is only slight disruption to the strip for substantially less adverse shear than necessary for linear stability, while for co-operative shear, there is major disruption to the strip. It is significant that the potential vorticity of the imposed flow necessary to create shear of a given value increases dramatically as the interaction range of the inversion operator decreases, making shear stabilization increasingly less likely. This implies an increased propensity for filaments to 'roll-up' into small vortices as the interaction range decreases, a finding consistent with many numerical calculations performed using the quasi-geostrophic model.

1. Introduction

In recent years the 'potential vorticity' of balanced motion has increasingly been used to diagnose, understand and model the dynamics of the atmosphere, the oceans, and other stably stratified fluid systems (e.g. Hoskins, McIntyre & Robertson 1985; Kurganskiy & Tatarskaya 1987; McIntyre & Norton 1991). It provides a hierarchy of dynamical models all governed by the advection of a quantity 'potential vorticity', hereinafter 'PV', that is (*a*) materially conserved in the absence of heating and friction, and (*b*) whose instantaneous configuration determines all other quantities in the system at that instant ('PV invertibility'). The simplest model in this hierarchy is two-dimensional incompressible vortex dynamics, hereinafter '2VD' (the PV being identified as the ordinary vorticity), and the next is quasi-geostrophic shallow-water dynamics ('QGSW'). Both of these models idealize the motion of a

single layer of a real stratified flow. More realistic models include the quasi-geostrophic multi-layer models ('QGML'), which like 2VD and QGSW have an inversion operator (giving the velocity in terms of the PV) that is linear. Further models in the hierarchy, such as the semi-geostrophic shallow-water and multi-layer models, use more accurate, nonlinear operators.

In the present state of knowledge, there is a need to learn more about how far the analogies between different models in the hierarchy can be carried, and where on the other hand the differences between them are significant. This question can be studied within the set of models having Green-function integral inversion operators that link the stream function to the potential vorticity, as well as a two-dimensional, non-divergent velocity field. These models exemplify some of the differences of interest, particularly those relating to the interaction range of the inversion operator, and in addition all these models possess standard Hamiltonian structure. (An elementary proof is to replace the inverse Laplacian by the Green-function inversion operator in the derivation given by McIntyre & Shepherd 1987, §7.) In 2VD the Green function is logarithmic in the vortex separation r, which represents a relatively long interaction range. At the opposite extreme, the Green function in QGSW represents a relatively short interaction range. It has an exponential tail, scaling with the Rossby length L_R, the lengthscale based on the Coriolis parameter f_0 and the gravity wave speed. In the limit of continuous stratification QGML has a (three-dimensional) Green function that behaves like $1/r$ for large r.

Insight into the sensitivity of two-dimensional vortex motion to the form of the Green function of the flow will give us a better understanding of what aspects of single-layer models may be sufficiently robust to carry over to the real atmosphere and oceans. At present, single-layer models are the only ones that offer sufficient spatial resolution to come anywhere near adequately simulating the full dynamic range of the horizontal motion. This paper is part of a general study of how sensitive two-dimensional vortex interactions, much of whose phenomenology is familiar in the case of 2VD, are to the form of the Green function.

One of the most ubiquitous features of high-Reynolds-number two-dimensional or layerwise-two-dimensional flows is the presence of strips or filaments of PV. Strips of PV are formed in stratospheric models, see for instance the 2VD model of Juckes & McIntyre (1987), and their robustness is a critical issue. Thin strips of vorticity are also ubiquitous in numerical experiments of nonlinear 2VD flows at high Reynolds numbers (see for example Benzi, Patarnello & Santangello 1987; Dritschel 1988, 1989*a*; Legras, Santangello & Benzi 1988; Melander, McWilliams & Zabusky 1987; and Melander, Zabusky & McWilliams 1988), in laboratory experiments of two-dimensional flows (Couder & Basdevant 1986; Griffiths & Hopfinger 1987), as well as in stably stratified three-dimensional flows (Hedstrom & Armi 1988). These strips seldom roll up into strings of miniature vortices as the classic analysis of Rayleigh (1894) might lead one to believe. The explanation for the persistence of these strips is the stabilizing effect of the large-scale strain field associated with coherent vortices (Dhanak 1981; Dritschel 1989*b*; Dritschel *et al.* 1991). In the vicinity of intense coherent vortices, where most of the filamentary vorticity is produced via interactions with other vortices, the differential rotation causes the filaments to rapidly align with the circulating flow, and then shear is the prime factor affecting stability (Dritschel 1989*b*; hereinafter referred to as D). In this paper, we re-examine the stability of filaments in shear, widening the scope to models with arbitrary Green functions $G(r)$.

In the next section, the stability of a straight strip of uniform PV with imposed

background shear, that also has uniform PV, is derived for arbitrary $G(r)$. In all models in which the velocity due to the strip is finite, it is shown that the strip can be stabilized by imposed shear that reverses the total shear across the strip, as in 2VD. If, additionally, $G(r)$ decays fast enough, the strip can also be stabilized by shear having the same sense as the shear of the strip – this does not occur in 2VD. The stability of thin circular strips is also examined, since in reality the strips whose stability is in question encircle intense coherent vortices; however, the effects of curvature are found to be truly insignificant for thin strips, as found in the 2VD model (see D). Results for specific models are given in the following sections; in §3 the established results for 2VD are rederived from the general formula developed in §2, in §4 new results are derived for the QGSW model, and in §5 new results are derived for a class of models having a Green function characterized by algebraic decay at large separations. Inter-model comparisons highlight important similarities, differences and trends. Section 6 connects shear stabilization to generalized forms of Arnol'd's stability theorems (Arnol'd 1965, 1966). Nonlinearity is considered for the first time in §7. The evolution of disturbed strips in both the 2VD and QGSW models is calculated with a contour-dynamics model. A number of significant differences between linear and nonlinear evolution are observed even at small disturbance amplitude, indicating enhanced stability for strips in adverse shear and lack of stability for strips in co-operative shear.

2. Stability of a strip of potential vorticity

In this section we present general conditions and results for the linear stability of a straight strip of PV in a background shear flow. For a region of constant potential vorticity q embedded in an irrotational flow, the velocity field is determined by the contour integral

$$\boldsymbol{u}(\boldsymbol{x}) = -q \oint_{\mathscr{C}} G(r)\, \mathrm{d}\boldsymbol{x}', \tag{1}$$

where $G(r)$ is the Green function of the model, $\mathscr{C}$ is the boundary of the region and $r = |\boldsymbol{x}-\boldsymbol{x}'|$ (Dritschel 1989*a*).

We first consider the equilibrium configuration defined as a region of uniform potential vorticity q bounded by the two lines $y = \pm\frac{1}{2}\Delta$, beyond which the flow is irrotational. The flow due to the equilibrium configuration may be written as $\bar{\boldsymbol{u}} = (\bar{u}(y), 0)$ where

$$\bar{u}(y) = q \int_{-\infty}^{\infty} \{G([x^2+(y-\tfrac{1}{2}\Delta)^2]^{\frac{1}{2}}) - G([x^2+(y+\tfrac{1}{2}\Delta)^2]^{\frac{1}{2}})\}\, \mathrm{d}x, \tag{2}$$

i.e. the flow is parallel to the axis of the strip and independent of the position along the strip.

Linear stability is determined by adding small, normal-mode boundary disturbances of the form

$$\eta_{\pm}(x,t) = \mathrm{Re}\,[\tilde{\eta}_{\pm} \exp(\mathrm{i}kx - \mathrm{i}\sigma t)] \quad (k > 0) \tag{3}$$

to the upper and lower edges of the strip and linearizing the equations of motion $\mathrm{D}\boldsymbol{x}/\mathrm{D}t = \boldsymbol{u}(\boldsymbol{x})$ about $\boldsymbol{x} = \boldsymbol{x}_{\pm} \equiv (x, \pm\frac{1}{2}\Delta)$. This is all that is necessary, since equation (1) for $\boldsymbol{x}$ on $\mathscr{C}$ is a complete dynamical description for the flow. It is true that more general rotational (q-varying) disturbances have been omitted, but within linear

theory such disturbances would simply be passively advected. By direct manipulation we obtain two coupled equations in the complex amplitudes $\tilde{\eta}_\pm$,

$$[\hat{\sigma} - k(\mathscr{I}_1 - \mathscr{I}_0)]\,\tilde{\eta}_+ + k\mathscr{I}_2\,\tilde{\eta}_- = 0, \tag{4a}$$

$$[\hat{\sigma} + k(\mathscr{I}_1 - \mathscr{I}_0)]\,\tilde{\eta}_- - k\mathscr{I}_2\,\tilde{\eta}_+ = 0, \tag{4b}$$

where $\hat{\sigma} = \sigma/q$ is the dimensionless complex growth rate of the disturbance,

$$\mathscr{I}_0(\Delta) = 2\int_0^\infty [G(x) - G((x^2+\Delta^2)^{\frac{1}{2}})]\,\mathrm{d}x, \tag{5a}$$

$$\mathscr{I}_1(k) = 2\int_0^\infty G(x)\cos kx\,\mathrm{d}x, \tag{5b}$$

and

$$\mathscr{I}_2(k,\Delta) = 2\int_0^\infty G((x^2+\Delta^2)^{\frac{1}{2}})\cos kx\,\mathrm{d}x. \tag{5c}$$

Note that $\bar{u}_\pm = \pm q\mathscr{I}_0$ is the undisturbed velocity on the upper and lower edge of the strip, respectively. For the coupled equations (4) to have a non-trivial solution the eigenvalue $\hat{\sigma}$ is required to take the value

$$\hat{\sigma} = \pm k[(\mathscr{I}_1 - \mathscr{I}_0)^2 - \mathscr{I}_2^2]^{\frac{1}{2}}. \tag{6}$$

We now consider the effect of adding a background shear flow that has uniform PV to the above configuration. This shear flow can be considered to be the flow due to a strip of uniform potential vorticity Q, say, with width much greater than any other lengthscale involved in the flow, and hence the flow has the same y-dependence as the flow inside the undisturbed strip, cf. equation (2). The above equilibrium flow is then augmented by this shear flow. In particular, the equilibrium velocities at the edges of the strip now assume the values $\bar{u}_\pm = \pm q\mathscr{I}_0(1-\Lambda)$, where Λ is a dimensionless shear parameter proportional to $-Q/q$. Positive Λ corresponds to *adverse* shear as the background flow is opposing the flow due to the strip, while negative Λ corresponds to *co-operative* shear.

It is important to note that the relationship between the dimensionless shear Λ and the ratio of background to strip vorticity Q/q depends strongly on the Green function, and therefore a particular value of Λ will not correspond to the same value of Q/q for all Green functions.

The linear stability for the strip with background shear is obtained in precisely the same fashion as above. The resulting coupled equations and dispersion relation are the same as (4) and (6) with $\mathscr{I}_0$ replaced by $\mathscr{I}_0(1-\Lambda)$, i.e. the complex growth rate is given by

$$\hat{\sigma} = \pm k[(\mathscr{I}_1 - \mathscr{I}_0(1-\Lambda))^2 - \mathscr{I}_2^2]^{\frac{1}{2}}. \tag{7}$$

To simplify the following analysis we assume that the Green function $G(r)$ is such that

$$\left.\begin{aligned} &\text{(i)}\ G(r) \to -\infty \quad \text{as} \quad r \to 0, \\ &\text{(ii)}\ G'(r) > 0, \quad G''(r) < 0, \\ \text{and} \quad &\text{(iii)}\ \mathscr{I}_0, \quad \mathscr{I}_1, \quad \text{and} \quad \mathscr{I}_2 \text{ are finite.} \end{aligned}\right\} \tag{8}$$

Condition (iii) is applied so that there are no infinite terms in the dispersion relation (7).

The condition that $\mathscr{I}_0$, and that therefore the basic velocity on the edges of the strip, be finite implies that

$$rG(r) \to 0 \quad \text{as} \quad r \to 0, \tag{9}$$

see Appendix A. In the remainder of this analysis we assume that $G(r)$ satisfies (9).

The strip will be linearly stable to all disturbances of the form (3) if the growth rate has no imaginary part, i.e. if the quantity under the radical in the dispersion relation (7) is positive for all k. As $\mathscr{I}_0 < 0$ and $\mathscr{I}_1 < \mathscr{I}_2 < 0$ for any $G(r)$ satisfying (8), we have from (7) that the strip will be stable when

$$\Lambda \geqslant 1, \tag{10a}$$

or when

$$\Lambda \leqslant \Lambda_C(\Delta) = \min_{k \geqslant 0} \left\{ 1 - \frac{\mathscr{I}_1(k) + \mathscr{I}_2(k, \Delta)}{\mathscr{I}_0(\Delta)} \right\}. \tag{10b}$$

It is shown in Appendix A that the critical shear Λ_C is finite if

$$rG(r) \to 0 \quad \text{as} \quad r \to \infty, \tag{11}$$

and then

$$\Lambda_C = \frac{2\mathscr{I}_2(0, \Delta)}{\mathscr{I}_2(0, \Delta) - \mathscr{I}_1(0)} < 0. \tag{12}$$

Therefore in all models with a Green function less singular than $1/r$ the strip may be stabilized by adverse shear (condition (10*a*)), while if the Green function also decays faster than $1/r$ for large r the strip may be also stabilized by co-operative shear (condition (10*b*)).

The above instabilities are caused by the same mechanism as that responsible for barotropic and baroclinic instabilities (see §6 of Hoskins *et al.* 1985). The flow associated with the waves on each edge of the strip causes the waves to propagate against the basic flow associated with the undisturbed strip. For particular phase relationships between the waves on the edges, phase locking can occur and the waves amplify (see Dritschel & Polvani 1991, §5, for a simple heuristic argument). Stabilization by adverse shear corresponds to the reversal of the direction of the basic flow on the two edges of the strip, making it impossible for the phase propagation to keep the waves stationary – a necessary condition for instability by the symmetry of the problem. As the stabilizing adverse shear is approached and the basic flow weakens, only short waves can phase-lock and amplify. In the case of co-operative shear, the magnitude of the basic flow is augmented by the shear (in fact $\bar{u}_\pm \to \mp\infty$ as $\Lambda \to -\infty$). If the Green function satisfies both conditions (9) and (11), there exists a maximum phase speed with which waves can propagate relative to the basic flow and therefore a value of co-operative shear Λ_C less than that for which the basic flow outruns the phase propagation of all waves. Hence stabilization by co-operative shear occurs when the wave-induced velocity field is too weak to hold the waves stationary against the basic flow.

To determine the dependence of the above results on the vorticity distribution, they have been extended to non-uniform vorticity distributions. If we consider, as an approximation of a continuous PV distribution, a cross-strip distribution consisting of m discrete steps in PV, the set of coupled equations for the disturbance amplitude at each interface can be determined by linear superposition of the results for a single strip of uniform PV. The resulting eigenvalue problem can be solved to determine the $2m$ eigenvalues σ corresponding to the phase speeds and growth rates of $2m$ distinct modes. See D, §3, for details of the stability of a strip with non-uniform vorticity, in 2VD.

Circular strips are considered next, in part because strips take on a progressively more circular shape when wound around intense coherent vortices (which also provide a source of stabilizing shear), and in part because there is a surprisingly close connection between the stability of circular and straight strips. By a judicious choice

of geometrical correspondence, we show below that the circular and straight strip stability results can be brought into numerically close correspondence except for unusually wide circular strips (improving even on the 2VD results of Zakharov 1977 and D).

We suppose in the following that the strip has a negligible effect on the enclosed vortex. This allows one to replace the enclosed vortex by a point vortex of the same circulation (see D for justification). We consider a circular strip of constant potential vorticity q, bounded inside by the circle $r = a$ and outside by the concentric circle $r = b$, with a point vortex of circulation Γ at the origin. Situating the point vortex at the origin adds a potentially stabilizing shear flow to the circular strip. From (1), we have that the velocity due to the circular strip is wholly azimuthal, $\bar{\boldsymbol{u}} = \bar{u}_\theta \hat{\boldsymbol{e}}_\theta$, and the angular velocity is

$$\Omega_s(r) = q(\mathscr{F}(a,r) - \mathscr{F}(b,r)) \equiv q\alpha_s(r), \tag{13}$$

where

$$\mathscr{F}(r_1, r_2) = \frac{r_1}{r_2} \int_0^{2\pi} G((r_1^2 + r_2^2 - 2r_1 r_2 \cos\phi)^{\frac{1}{2}}) \cos\phi \, \mathrm{d}\phi. \tag{14}$$

The linear stability of small radial boundary disturbances

$$\eta_\pm(\theta, t) = \mathrm{Re}\,[\tilde{\eta}_\pm \exp(\mathrm{i}m\theta - \mathrm{i}\sigma t)] \quad (m = 1, 2, \ldots)$$

to the outer and inner interface is again found from the linearized velocity and kinematic condition at each vorticity interface. The growth rates are obtained by solving the eigenvalue problem

$$[\sigma - m\Omega(b) - q\mathscr{K}_{bb}]\tilde{\eta}_+ + q\mathscr{K}_{ab}\tilde{\eta}_- = 0, \tag{15a}$$

$$[\sigma - m\Omega(a) + q\mathscr{K}_{aa}]\tilde{\eta}_- - q\mathscr{K}_{ba}\tilde{\eta}_+ = 0, \tag{15b}$$

where $\mathscr{K}_{ab} \equiv \mathscr{K}_m(a, b)$ and

$$\mathscr{K}_m(r_1, r_2) = \frac{mr_1}{r_2} \int_0^{2\pi} G((r_1^2 + r_2^2 - 2r_1 r_2 \cos\phi)^{\frac{1}{2}}) \cos m\phi \, \mathrm{d}\phi. \tag{16}$$

To enable the closest possible comparison of the stability results with those of the straight strip, we want the inner and outer edges of the circular strip to be rotating at an equal but opposite rate, and the velocity difference across the strip to be equal to that in the straight case. This is achieved by requiring

$$\Omega(b) = -\Omega(a) = \Omega_0 \tag{17a}$$

with

$$\Omega_0 = \frac{-\bar{u}_+}{\frac{1}{2}(a+b)} = -\frac{2q\mathscr{I}_0(\Delta)(1-\Delta)}{a+b} \equiv q\hat{\Omega} \tag{17b}$$

(where $\bar{u}_+$ is the velocity on the upper edge of the straight strip, $\Delta = b - a$ and $\mathscr{I}_0$ is defined by (5a)) and then by altering the basic flow slightly to include a uniform background potential vorticity δq and a modified point vortex strength $\delta\Gamma$. The values of δq and $\delta\Gamma$ are determined in Appendix B.

Note that the dimensionless shear parameter Δ appearing in (17b) for $\hat{\Omega}$ equals

$$\Delta = \frac{1}{f(a,b)} \frac{\Gamma}{q\pi a^2}, \tag{18}$$

where $f(a, b)$ depends on the Green function. In 2VD, $\Delta = \Gamma/q\pi a^2$, which is the ratio of the point-vortex circulation to the circulation of a disc of radius a and PV value q.

From the eigenvalue problem (15), we have that the dimensionless growth rate $\hat{\sigma} \equiv \sigma/q$ is given by

$$\hat{\sigma} = \tfrac{1}{2}\{(\mathscr{K}_{bb}-\mathscr{K}_{aa}) \pm [(\mathscr{K}_{bb}-\mathscr{K}_{aa})^2+4(\mathscr{K}_{aa}+m\hat{\Omega})(\mathscr{K}_{bb}+m\hat{\Omega})-4\mathscr{K}_{ab}\mathscr{K}_{ba}]^{\frac{1}{2}}\}. \quad (19)$$

Instability requires a non-zero imaginary part to $\hat{\sigma}$ so the quantity under the radical must be negative in this case. This occurs when $\Lambda_C < \Lambda < 1$ ($\Lambda_C < 0$ and depends on the Green function). Thus, like the straight strip, the circular strip may be stabilized by both adverse and co-operative shear.

In Appendix C, it is verified that the dispersion relation for a thin circular strip, $\Delta = b-a \ll a$, reduces to that for a straight strip, upon identifying $k = m/a$, and this is corroborated by the quantitative results given below.

3. The classical 2VD model

The stability of an isolated straight strip of uniform vorticity in two-dimensional vortex dynamics (2VD) was first studied by Rayleigh (1894). Recent extensions include non-uniform vorticity distributions, annular geometry and the effects of a central point vortex (Zakharov 1977; D). In this section we show that these stability results can be derived from the general formula given in the previous section. For detailed discussion of these stability results, reference should be made to the above studies.

The materially conserved PV in 2VD is just the ordinary vorticity of the flow (i.e. $q = \omega = \nabla^2\psi$) and the Green function is

$$G(r) = \frac{1}{2\pi}\log r. \quad (20)$$

For a straight strip of uniform vorticity ω the equilibrium flow due to the strip is $\bar{u} = \mp\frac{1}{2}\omega\Delta$ above and below the strip respectively, and $\bar{u} = -\omega y$ inside the strip (cf. (2)). The background shear flow is then of the form $\Lambda\omega y$, which corresponds to adding uniform background vorticity $Q = -\Lambda\omega$. From (7) we have that the complex growth rate $\hat{\sigma}$ is given by the dispersion relation

$$\hat{\sigma} = \pm\tfrac{1}{2}\{[1-k\Delta(1-\Lambda)]^2-\mathrm{e}^{-2k\Delta}\}^{\frac{1}{2}} \quad (21)$$

(cf. D, equation (6)). Note that the integrals $\mathscr{I}_1$ and $\mathscr{I}_2$ given by (5) are infinite, but in deriving (4) we could have omitted at the outset the singular parts of these integrals by integrating (1) by parts; this exception only occurs when $G(r)$ does not decay with large r.

We now re-examine the case of a circular strip of uniform vorticity, previously considered by Zakharov (1977) and D. In D, it was proven that the stability of a thin circular strip reduces to that of a straight strip in the limit. This itself is not so surprising except for the fact that the imposed shear is irrotational in one case and rotational in the other. Here, we intend to show that the quantitative results can be brought into an even closer correspondence by a judicious choice of the annular flow.

As discussed in the previous section, to bring about the closest possible correspondence between the straight and circular strips, we add uniform background vorticity $\delta\omega$ (equivalent to moving to a rotating frame of reference in 2VD) and incrementing the central point-vortex strength by $\delta\Gamma$ (see Appendices B and D for details). From (19), the growth rates of small disturbances on the strip are given by

$$\hat{\sigma} = \pm\frac{1}{2}\left\{\left[1-\frac{2\Delta m}{a+b}(1-\Lambda)\right]^2-\left(\frac{a}{b}\right)^{2m}\right\}^{\frac{1}{2}}, \quad (22)$$

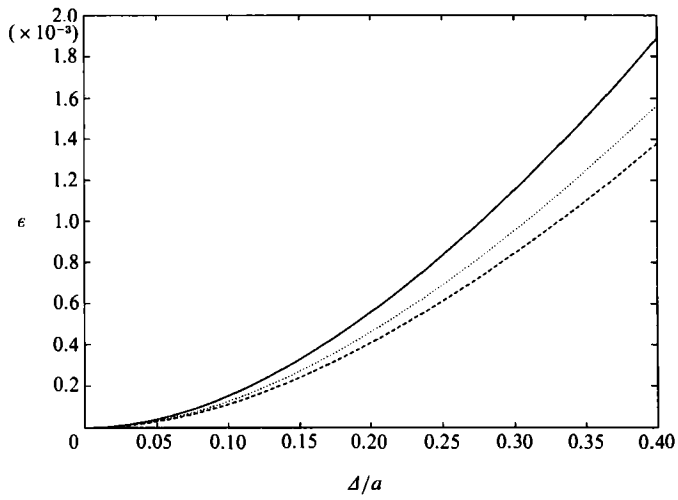

FIGURE 1. Difference between maximum dimensionless growth rate for a circular and straight strip $\epsilon = |\mathrm{Im}\,\hat{\sigma}_c - \mathrm{Im}\,\hat{\sigma}_s|$ versus dimensionless strip width Δ/a, for a 2VD strip with no shear $\Lambda = 0$ (solid line), adverse shear $\Lambda = 0.5$ (dotted line), and co-operative shear $\Lambda = -0.5$ (dashed line).

where the dimensionless shear is $\Lambda = \Gamma/\omega\pi a^2$. This formula differs from Zakharov (1977) and D.

In both the straight and circular cases, the strip is stable for all disturbances only when the adverse shear Λ is greater than or equal to unity (in agreement with the analysis of §2, as the Green function (20) decays slower than $1/r$ and so there is no stabilizing co-operative shear). The formula (22) gives numerical values very close to those for the straight strip (identifying $k = m/a$) even for moderately thick circular strips – see figure 1 which plots the difference in the maximum growth rate between the circular and straight cases as a function of the relative strip width Δ/a. This result confirms that the essential mechanism controlling stability is imposed shear. As stated in D, it is irrelevant whether it be rotational or irrotational.

4. The QGSW model

We next present new results for a strip of PV in the quasi-geostrophic shallow-water model, and investigate the sensitivity of the above stability results to the interaction range of the model. In the QGSW model the PV is related to the stream function by $q = \nabla^2\psi - \gamma^2\psi$, and the Green function is

$$G(r) = -\frac{1}{2\pi}K_0(\gamma r), \tag{23}$$

where K_0 is the modified Bessel function of zeroth order and γ is the inverse of the radius of deformation L_R. The radius of deformation is defined as $L_R^2 = gH/f_0^2$, where g is the acceleration due to gravity, H is the depth of fluid and f_0 is the Coriolis parameter. For small separations compared with the radius of deformation, $r \ll L_R$, this function is the same as the 2VD Green function (20), but for large separations, $r \gg L_R$, it falls off exponentially, $G \approx -\mathrm{e}^{-\gamma r}/(8\pi\gamma r)^{\frac{1}{2}}$.

For a straight strip of uniform potential vorticity q, the undisturbed flow above and below the strip is $\bar{u} = \mp q\gamma^{-1}\sinh(\gamma\Delta/2)\,\mathrm{e}^{\mp\gamma y}$, respectively, and

$$\bar{u} = -q\gamma^{-1}\,\mathrm{e}^{-\gamma\Delta/2}\sinh(\gamma y)$$

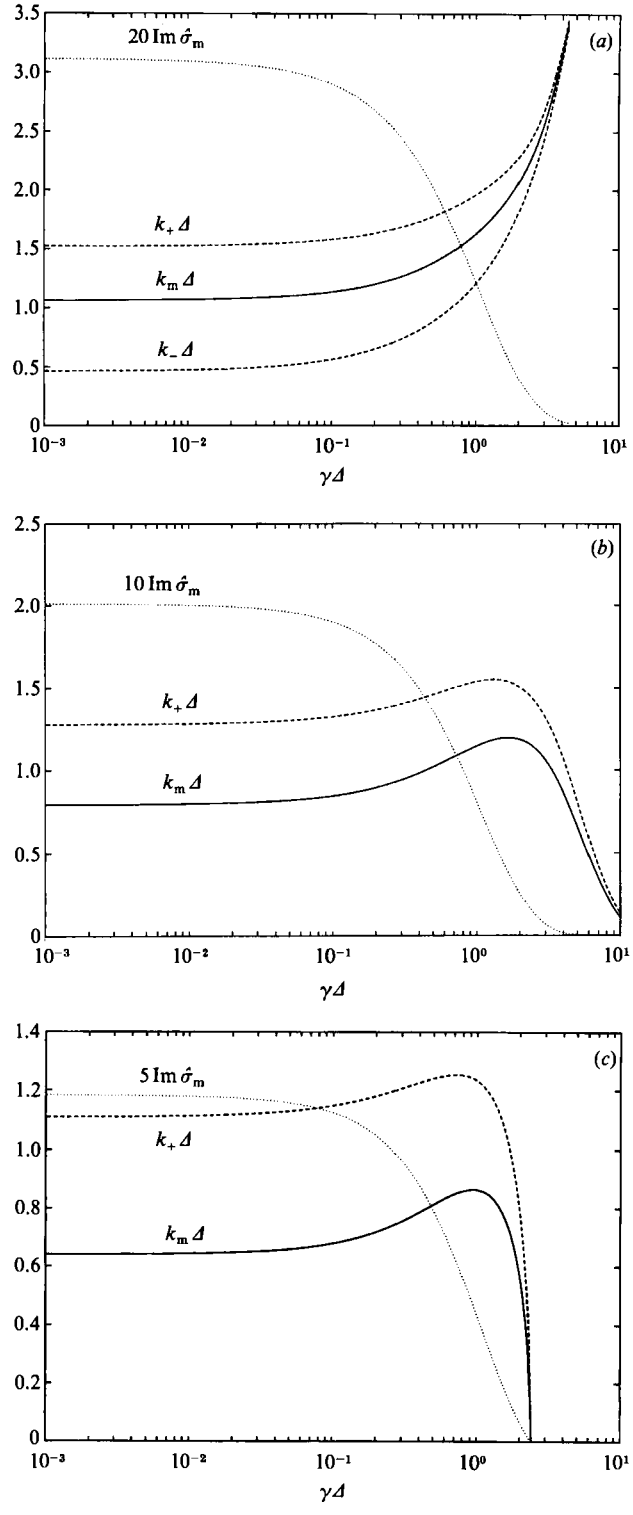

FIGURE 2. Maximum dimensionless growth rate $\mathrm{Im}\,\hat{\sigma}_m$, wavenumber $k_m\Delta$ of maximum instability, and range of unstable wavenumber $(k_-\Delta, k_+\Delta)$ versus dimensionless inverse radius of deformation $\gamma\Delta$ for a strip of PV in the QGSW model. (*a*) Adverse shear $\Lambda = 0.2$, (*b*) no shear $\Lambda = 0$, and (*c*) co-operative shear $\Lambda = -0.2$. Note that $k_-\Delta = 0$ in (*b*) and (*c*).

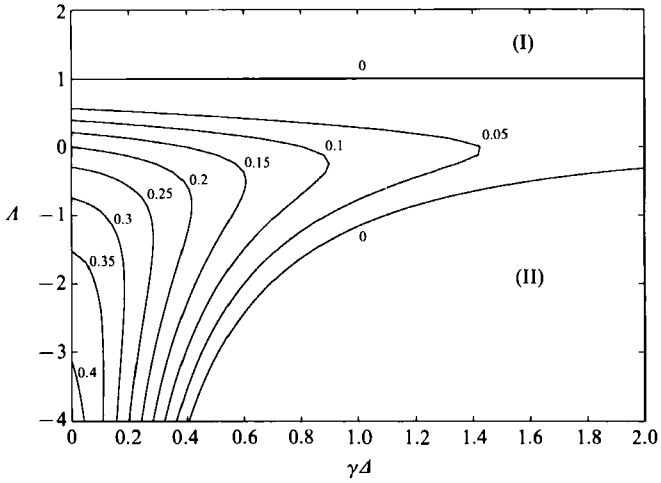

FIGURE 3. Contour plot of growth rate $\mathrm{Im}\,\hat{\sigma}$ versus inverse of radius of deformation $\gamma\Delta$ and shear Λ, for a strip of PV in the QGSW model. Regions (I) and (II) are stable.

inside. The background shear flow is then $\Lambda q\gamma^{-1}\mathrm{e}^{-\gamma\Delta/2}\sinh(\gamma y)$, corresponding to a uniform background potential vorticity $Q = \Lambda q\,\mathrm{e}^{\gamma(D-\Delta)/2}$ (D is a distance much greater than both the strip width Δ and the radius of deformation L_R – note the exponential dependence). From (7), together with (23), the dispersion relation is

$$\hat{\sigma} = \pm\frac{1}{2}\frac{k}{\lambda}\left\{\left[1-\frac{\lambda}{\gamma}(1-\mathrm{e}^{-\gamma\Delta})(1-\Lambda)\right]^2 - \mathrm{e}^{-2\lambda\Delta}\right\}^{\frac{1}{2}}, \tag{24}$$

where $\lambda = (k^2+\gamma^2)^{\frac{1}{2}}$.

As expected from the form of the Green function (23), the equilibrium flow and the dispersion relation are the same as those for 2VD in the limit of large radius of deformation, or $\gamma\Delta \ll 1$. As seen in figure 2, the maximum growth rate (over wavenumber k), $\mathrm{Im}\,\hat{\sigma}_\mathrm{m}$, diminishes with increasing $\gamma\Delta$, reflecting the shortening interaction range of the Green function.

From the dispersion relation (24), the strip will be stable for adverse shear

$$\Lambda \geqslant 1$$

or for co-operative shear $\qquad \Lambda \leqslant \Lambda_\mathrm{C} = \dfrac{-2\,\mathrm{e}^{-\gamma\Delta}}{1-\mathrm{e}^{-\gamma\Delta}}.$

Λ_C is finite because the Green function (23) falls off quicker than $1/r$ (see §2), and the value of Λ_C may be calculated using (12). The behaviour of $\mathrm{Im}\,\hat{\sigma}_\mathrm{m}$ as a function of the two dimensionless parameters $\gamma\Delta$ and Λ is illustrated in figure 3. Note again the dramatic decrease in growth rate as the radius of deformation becomes smaller than the strip width; growth rates remain less than 1% of the strip's PV for $L_\mathrm{R} < \frac{1}{2}\Delta$.

The stability of strips with non-uniform PV is considered next. Figure 4 is a plot of the maximum dimensionless growth rate $\mathrm{Im}\,\hat{\sigma}_\mathrm{m}$ and the corresponding dimensionless wavenumber $k_\mathrm{m}\Delta$ as a function of Λ, for $\gamma\Delta = 1$ and for the same three distributions used by D (plots for different values of $\gamma\Delta$ show similar behaviour). The general shape of the growth rate curves is similar for all three cross-strip distributions, with all distributions being stabilized by adverse and co-operative shear. The rough variation in the curves as Λ approaches unity is due to the competition between the various modes of instability having different internal structure. The wavenumber of maximum instability $k_\mathrm{m}\Delta$ also shows little dependence on the PV distribution,

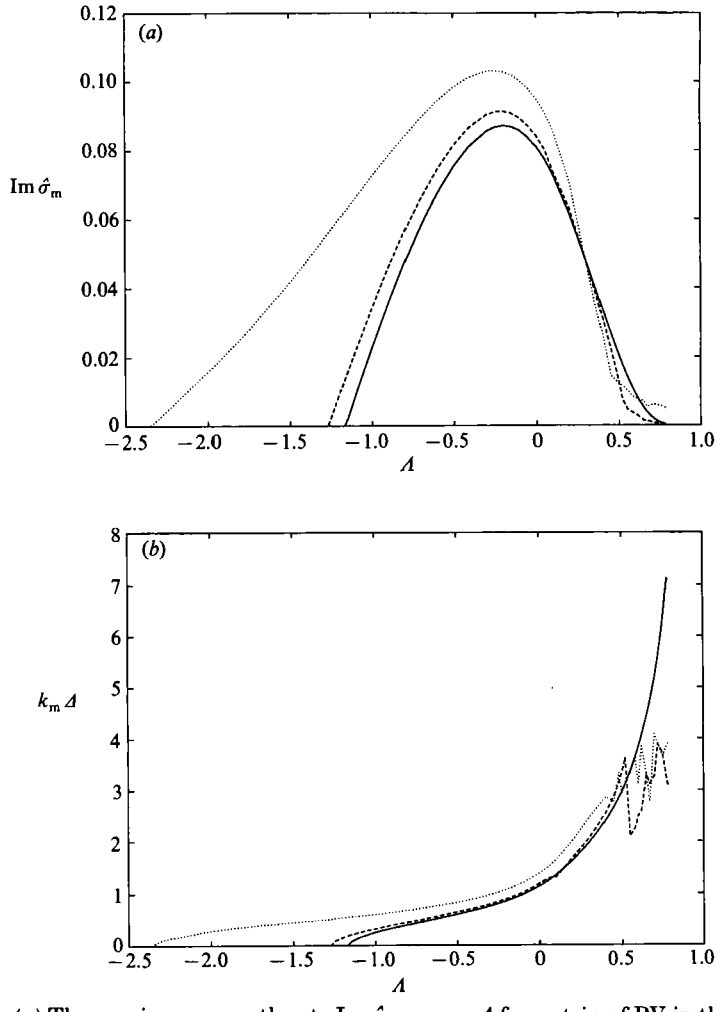

FIGURE 4. (*a*) The maximum growth rate Im $\hat{\sigma}_m$ versus Λ for a strip of PV in the QGSW model with $\gamma\Lambda = 1$, for the three cross-strip profiles $\epsilon = 0$ (solid line), $\epsilon = 0.2$ (dashed line), $\epsilon = 0.5$ (dotted line) of D. (*b*) The wavenumber $k_m \Lambda$ of maximum instability versus Λ for the three cross-strip profiles in (*a*).

except near $\Lambda = 1$ where unstable modes have short wavelengths and therefore strongly sense the non-uniformity in PV. As in 2VD, stability depends almost entirely on the peak (potential) vorticity within the strip, and relatively little on the precise distribution of PV.

We now consider the stability of a thin circular strip of potential vorticity, and compare the results with those of a straight strip. Following the analysis of §2, we add a uniform background potential vorticity δq and augment the point-vortex strength by $\delta\Gamma$ so that the edges of the strip rotate at the same rate but in opposite directions, and the velocity difference across the strip corresponds to that of the straight strip (see Appendices B and D for the values of δq and $\delta\Gamma$). Unlike in 2VD, a uniform background PV is not the same as moving to a rotating frame of reference: the flow inside a large circular vortex of uniform PV is no longer rigid rotation. Instead, background PV sets up a variable rotation rate

$$\Omega_p(r) \propto \delta q I_1(\gamma r)/\gamma r.$$

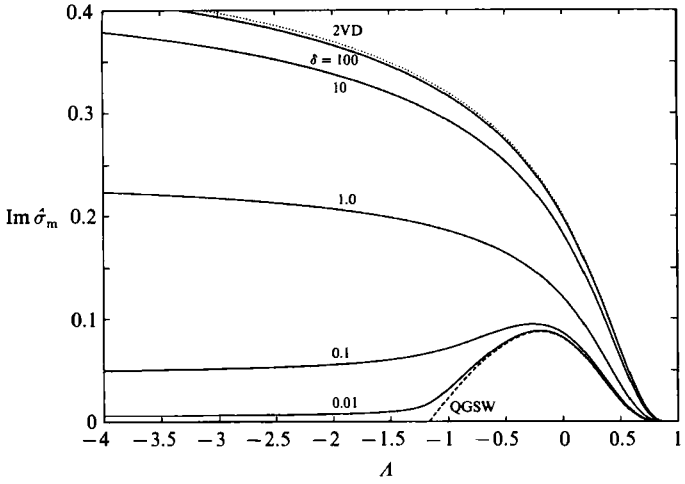

FIGURE 5. Maximum growth rate $\mathrm{Im}\,\hat{\sigma}_m$ as a function of Λ for a strip of PV with $\gamma\Lambda = 1$ in the QGSW model, the two-layer model with $\delta = 0.01, 0.1, 1.0, 10, 100$, and the 2VD model.

Stability is determined from the dispersion relation (19), with coefficients $\mathscr{K}_m$ as in Appendix D. There are no surprises. For large radius of deformation, the 2VD results are recovered, and overall there is a very close correspondence between the circular and straight strip results.

What is more interesting is the circulation of the point vortex required for adverse-shear stabilization ($\Lambda \geqslant 1$). From (18), the circulation of the point vortex must satisfy

$$\Gamma \geqslant q\pi a^2 f(\gamma a, \Lambda/a).$$

The function f is insensitive to Λ/a for thin strips, but increases exponentially with γa, $f \approx (2/\pi)^{\frac{1}{2}}(\gamma a)^{-\frac{3}{2}}\mathrm{e}^{\gamma a}$ for $\gamma a \gg 1$. Therefore, as the interaction range of the Green function decreases γa increases and the point-vortex circulation required to bring about stabilization by adverse shear increases exponentially. This is the first indication that strips of PV may not be easily stabilized in the QGSW model.

Finally in this section, we discuss the stability of a strip of PV in the upper layer of the two-layer quasi-geostrophic model (Phillips 1954). When there is no PV in the lower layer of the model the Green function for the motion in the upper layer is given by

$$G(r) = \frac{\delta}{1+\delta}\log r - \frac{1}{1+\delta}K_0(\bar{\gamma}r), \tag{25}$$

where $\bar{\gamma} = \gamma(1+\delta)^{\frac{1}{2}}$, γ is the inverse of the local deformation radius, and δ is the ratio of the thicknesses of the upper and lower layers. Note that (25) is just a linear combination of the Green functions for the 2VD and the QGSW models (it reduces to the 2VD Green function in the limit $\delta \to \infty$, and to the QGSW Green function when $\delta \to 0$). The stability analysis for a strip with uniform PV is as described in §2 with the integrals $\mathscr{I}_0$, $\mathscr{I}_1$, and $\mathscr{I}_2$ being the same linear combination of the respective integrals in the 2VD and QGSW models.

Figure 5 plots the maximum dimensionless growth rate $\mathrm{Im}\,\hat{\sigma}_m$ as a function of dimensionless shear Λ, with $\gamma\Lambda = 1$, for several values of δ. The most significant difference between the results for the two-layer model and the QGSW model ($\delta = 0$) is that the strip is no longer stabilized by co-operative shear. This is because for large r the Green function (25) behaves logarithmically for non-zero δ, rather than falling

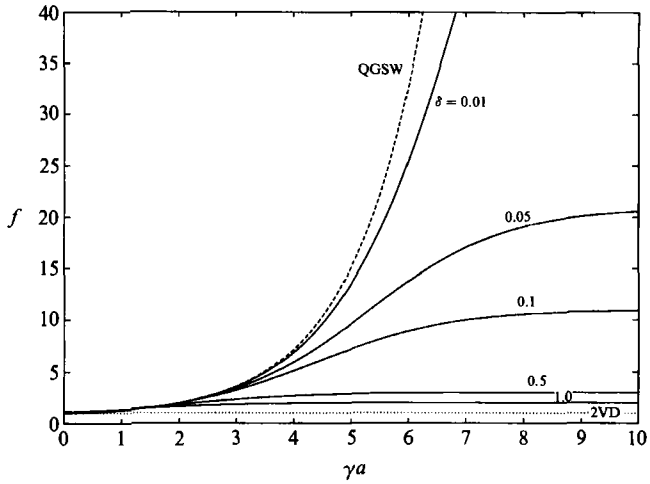

FIGURE 6. The function $f = \Gamma/q\pi a^2 \Lambda$ versus inverse radius of deformation γa for the QGSW model, the two-layer model with $\delta = 0.01$, 0.05, 0.1, 0.5, 1.0, and the 2VD model.

off exponentially, and therefore does not satisfy condition (11) (and hence a finite Λ_C does not exist). For given Λ, the maximum growth rate decreases with δ, but the ratio f of the shear PV to the strip PV which produces this value of Λ increases with decreasing δ (see figure 6). The ratio tends to the finite value $(1-\delta)/\delta$ in the limit of $\gamma\Lambda \to \infty$ since the logarithmic part of (25) then dominates.

5. Hybrid models

In this section we consider hybrid models which have Green functions which are logarithmic for small separations but fall off algebraically for large r. First, we consider the Green function

$$G(r) = \frac{1}{4\pi}\log\left(\frac{r^2}{r^2+L^2}\right), \tag{26}$$

where L is some lengthscale (the radius of deformation, say). Like the QGSW Green function (23) this function is logarithmic for small separations, $r \ll L$, but behaves like $L^2/4\pi r^2$ for $r \gg L$.

For (26), the dispersion relation (7) is

$$\hat{\sigma} = \pm\tfrac{1}{2}\{[1-e^{-kL}-k[\Lambda+L-(\Lambda^2+L^2)^{\frac{1}{2}}](1-\Lambda)]^2-[e^{-k\Lambda}-e^{-k(\Lambda^2+L^2)^{\frac{1}{2}}}]^2\}^{\frac{1}{2}}. \tag{27}$$

Qualitatively this dispersion relation has the same features as the QGSW one. In the limit $L/\Lambda \to \infty$ the growth rates are the same as in 2VD, while for $L/\Lambda \to 0$ the growth rates are practically negligible.

In agreement with the analysis of §2, the strip is stabilized for adverse shear

$$\Lambda \geqslant 1$$

or for co-operative shear

$$\Lambda \leqslant \Lambda_C = \frac{2[\Lambda-(\Lambda^2+L^2)^{\frac{1}{2}}]}{\Lambda+L-(\Lambda^2+L^2)^{\frac{1}{2}}}.$$

As with the QGSW model, the critical co-operative shear Λ_C tends to infinity in the 2VD limit, $L/\Lambda \to \infty$, and tends to zero in the limit $L/\Lambda \to 0$ (note that for $L/\Lambda \ll 1$, $\Lambda_C \approx -L/\Lambda$ compared with $\Lambda_C \approx -2e^{-\Lambda/L}$ in the QGSW model). Figure 7 is the contour

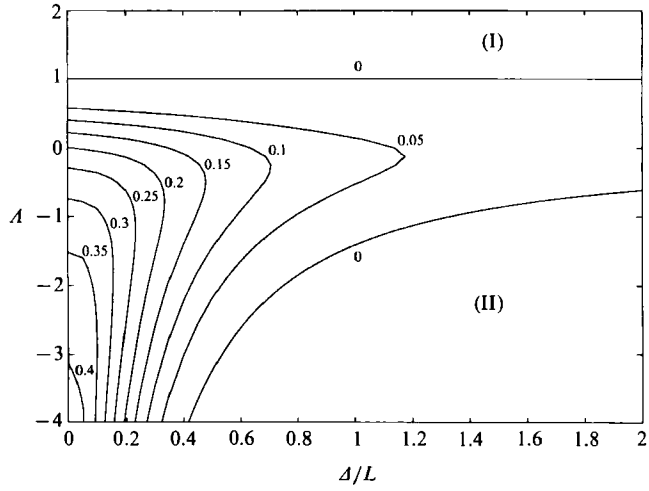

FIGURE 7. As in figure 3, but with the hybrid Green function (26).

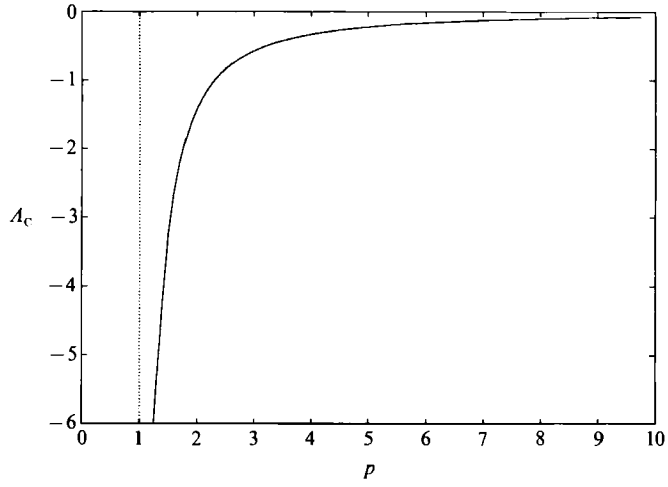

FIGURE 8. The stabilizing co-operative shear Λ_c versus the algebraic power p of the hybrid Green function (28) for a strip with $\Delta = L$.

plot of maximum growth rate for given shear Λ and ratio Δ/L for the Green function (26). The growth rate and the magnitude of the critical co-operative shear for given Δ/L are slightly larger than in QGSW (cf. figure 3), but the overall behaviour is very similar, with the growth rate decreasing rapidly as $\Delta/L \to 0$.

The Green function (26) is a member of the general family

$$G(r) = -\frac{1}{2p\pi}\log\left(\frac{r^p}{r^p + L^p}\right) \quad (p > 0). \tag{28}$$

These Green functions are logarithmic for small separations, $r \ll L$ and they fall off like $1/r^p$ for large separations, $r \gg L$.

From the analysis of §2 we have that, for all members of this family, the strip can be stabilized by adverse shear; however, only when $p > 1$ can the strip be stabilized by co-operative shear too. Figure 8 shows the variation of Λ_c (calculated numerically from (12)) with p, for $\Delta/L = 1$. This shows that the critical value of stabilizing co-

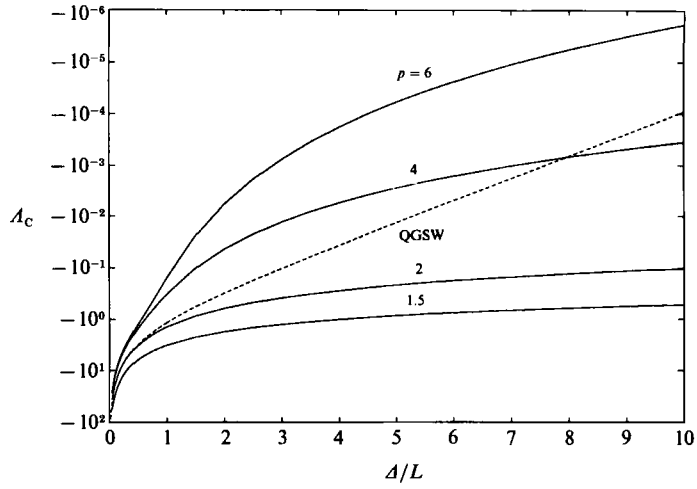

FIGURE 9. The stabilizing co-operative shear Λ_C versus Δ/L for the hybrid Green function (28) with $p = 1.5$, 2, 4, 6, and for the QGSW model.

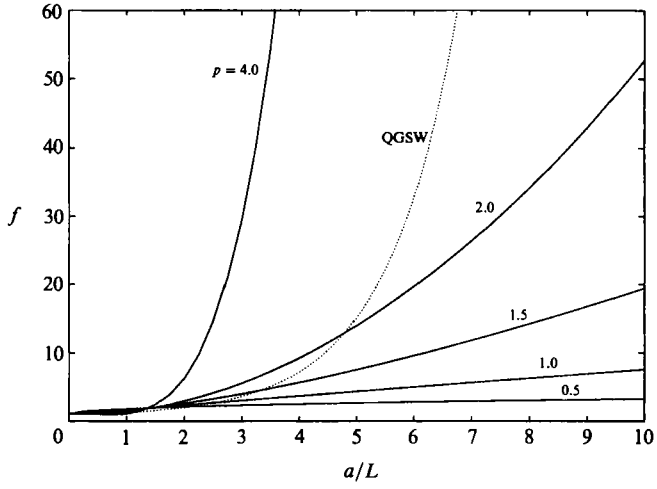

FIGURE 10. Function $f = \Gamma/q\pi a^2\Lambda$ versus a/L for the hybrid Green function (28) with $p = 0.5$, 1, 1.5, 2, 4, and for the QGSW model.

operative shear decreases as the interaction range of the Green function decreases, i.e. $\Lambda_C \to 0$ as $p \to \infty$. The variation of Λ_C with Δ/L for several values of p (and for the QGSW model) is shown in figure 9. As the interaction range of the Green function decreases (either increasing p or decreasing L) the stabilizing shear Λ_C decreases, implying a greater range of stability.

The ratio of shear PV to the strip PV necessary for stability varies with p and L. For a circular strip the ratio of the circulations of the point vortex and strip necessary for stability ($\Lambda = 1$) is given by the function f defined in (18). f has the same dependence with L/a as the Green function with r for large r, $f \propto (a/L)^p$, see figure 10. Hence, as in the QGSW model, a progressively stronger point vortex is necessary for stabilization as the interaction range of $G(r)$ decreases.

6. Sufficient conditions for stability

The first stability theorem of Arnol'd (1965, 1966) holds for all the Green functions considered in §§4 and 5 (this follows from the Hamiltonian structure of these models). For straight strips of piecewise-constant PV the flow is stable if $\bar{u}_j \tilde{q}_j \geqslant 0$ for all j ($\tilde{q}_j$ is the PV jump at $y = y_j$), while for circular strips the stability condition is $\bar{\Omega}_j \tilde{q}_j \leqslant 0$ for all j (see D, §5). These conditions are satisfied by the flows considered in §2 when the adverse shear is such that $\Lambda \geqslant 1$, which is the same as the linear stability condition for adverse shear derived by the normal-mode analysis in §2. Hence the condition for stabilization by adverse shear is equivalent to Arnol'd's first stability theorem.

Benzi *et al.* (1982) extended both of Arnol'd's theorems to the QGSW model, and showed that the second theorem becomes $\mathrm{d}\bar{\psi}/\mathrm{d}q \leqslant -L_{\mathrm{R}}^2$. For parallel flows this is equivalent to $\bar{u}L_{\mathrm{R}}^2 \geqslant \mathrm{d}^2\bar{u}/\mathrm{d}y^2$. This condition is never satisfied by a strip of constant PV, but it can hold for a strip with finite vorticity gradients. By considering a strip with the cross-strip PV distributions of D, §3, it can be shown that the co-operative shear required to satisfy the second theorem is much larger (in magnitude) than the stabilizing co-operative shear determined in the normal-mode analysis of §2. Hence the stabilizing co-operative Λ_{C} is not related to Arnol'd's second stability theorem.

7. Nonlinearity

The nonlinear evolution of the linearly unstable flows considered in the previous sections is now examined. We use the method of 'contour dynamics' to perform numerical calculations of the evolution of strips of uniform PV. This numerical technique is designed for piecewise-constant (potential) vorticity distributions, and can be used for any two-dimensional or multi-layer model with a Green function $G(r)$. For full details of this method and its extension 'contour surgery', see Dritschel (1989*a*).

The contour-dynamics algorithm implemented uses numerical quadrature to evaluate the part of the contour integral between nodes. This method is computationally faster than using explicit evaluation of the integral (as in Dritschel 1989*a*), but numerical instability occurs when nodes on different contours (or different sections of the same contour) approach each other (Dritschel 1986). Hence this method is inaccurate when small scales develop in the flow. Because of this inaccuracy the calculations in this section have been terminated when small scales develop.

To examine the nonlinear evolution of initially small, unstable disturbances on a straight strip of vorticity in 2VD, D used the periodic version of contour dynamics. Unfortunately, although the periodic counterpart of a general Green function $G(r)$ can be determined from the method of images, it is not known in closed form, and so the evolution of a straight strip would require unjustified computational effort. As it has been shown that the linear stability of a thin circular strip is essentially the same as that of a straight strip, one might expect the nonlinear evolution to be similar too, and for this we can use the original Green function at much reduced computational effort. Indeed, repeating the straight-strip calculations of D but in circular geometry, we observe very little difference (compare figure 11 with figure 3 of D).

We now examine the nonlinear evolution for a strip of PV in the QGSW model. The evolution of circular strips of uniform PV with $\gamma\Lambda = 1$ was calculated for several

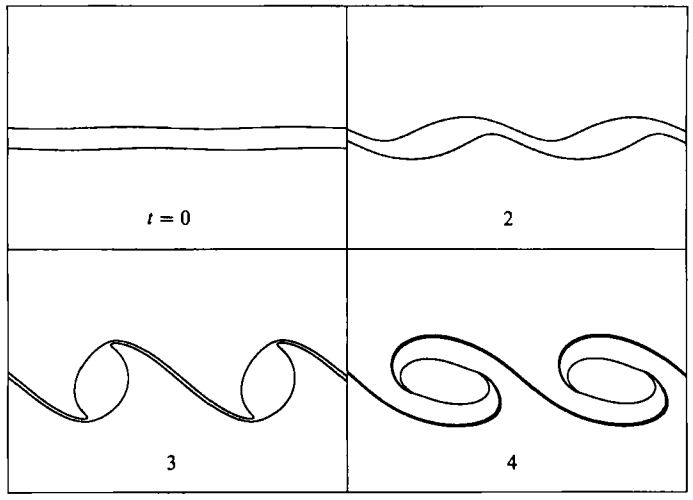

FIGURE 11. A contour-dynamics calculation of the instability of a circular strip of vorticity with no shear ($\Lambda = 0$) in the 2VD model ($a = 1, \Delta = 0.05, m = 16$). Radius versus angle is plotted for two periods of the disturbance. Time is shown on the plots.

Λ	Δ	m	$\mathrm{Im}\,\hat{\sigma}_s$	ϵ
−1.1	0.02	8	0.00915	3×10^{-5}
−0.9	0.05	7	0.03560	9×10^{-5}
−0.6	0.05	11	0.06749	4×10^{-5}
−0.3	0.05	16	0.08561	1×10^{-4}
0.0	0.08	15	0.08092	1×10^{-4}
0.05	0.08	16	0.07731	1×10^{-4}
0.10	0.10	14	0.07274	2×10^{-4}
0.15	0.10	16	0.06740	6×10^{-4}
0.20	0.11	17	0.06128	1×10^{-4}
0.25	0.11	17	0.05844	1×10^{-4}
0.26	0.11	17	0.05348	6×10^{-4}
0.27	0.11	18	0.05211	2×10^{-4}
0.28	0.11	18	0.05072	1×10^{-4}
0.30	0.11	19	0.04744	1×10^{-4}
0.35	0.12	19	0.04080	2×10^{-4}
0.40	0.12	21	0.03367	2×10^{-4}
0.43	0.12	23	0.02948	9×10^{-4}
0.44	0.12	23	0.02811	1×10^{-4}
0.45	0.15	19	0.02674	2×10^{-4}
0.50	0.15	21	0.02021	1×10^{-3}

TABLE 1. Strip width Δ and wavenumber m for calculations performed in the QGSW model. The radius of deformation L_R is equal to Δ in all calculations. ϵ is the difference between the maximum growth rate for a straight and a circular strip $\epsilon = |\mathrm{Im}\,\hat{\sigma}_s - \mathrm{Im}\,\hat{\sigma}_c|$, cf. figure 1.

different values of Λ. For each value of Λ, the inner and outer edges of a thin circular strip of uniform vorticity are disturbed by the most unstable eigenmode. The inner radius a is set at unity, the width of the strip $\Delta(\Lambda)$ is chosen so that the azimuthal wavenumber m corresponding to the most unstable mode is not too large, and the amplitude of the disturbance is 0.05Δ. The values of Δ and m used in each calculation are given in table 1. When $\gamma\Delta = 1$, the radius of deformation L_R of the Green function takes the same value as the strip width.

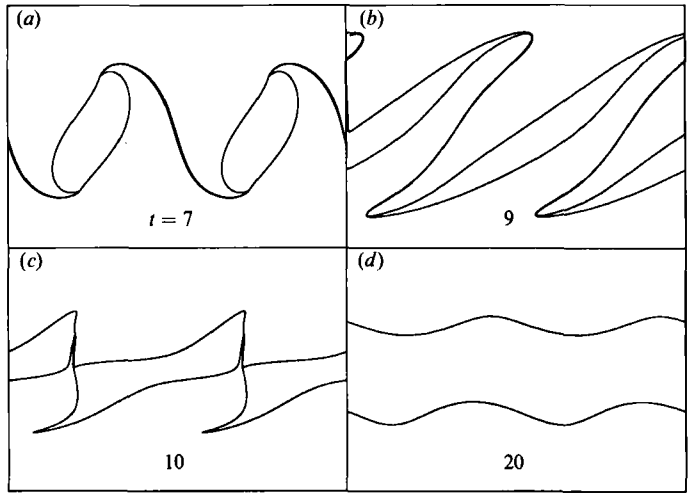

FIGURE 12. Final configuration of contour-dynamical calculations of the instability of a circular strip of PV with $\gamma\Lambda = 1$ in the QGSW model. (*a*) No shear $\Lambda = 0$, (*b*) $\lambda = 0.15$, (*c*) $\Lambda = 0.30$, and (*d*) $\Lambda = 0.45$. Refer to table 1 for further details.

For adverse shear, the behaviour is qualitatively the same as 2VD, compare figure 12 with figures 3–9 of D. As Λ increases towards unity there are four different regimes. For Λ less than 0.10 (approximately), the strip goes unstable and rolls up into a string of vortices. The second regime, in which the shear overcomes the initial roll-up and extends the vortices, occurs when $0.10 < \Lambda < 0.28$. For $0.28 < \Lambda < 0.44$, either vortices begin to form but are then torn in two, or thin filaments are shed from the interfaces. There is no disruption to the strip for adverse shear greater than 0.44 – this is substantially less than the value of unity necessary for linear stability. The corresponding regimes in 2VD are $\Lambda < 0.21$, $0.21 < \Lambda < 0.45$, $0.45 < \Lambda < 0.65$, and $0.65 < \Lambda$. For a more detailed description of the evolution in each regime (and numerical calculations) in 2VD, consult D. Although the values of Λ for each regime in QGSW are smaller than the corresponding 2VD values, the strength of the point vortex required for the same value of shear is much larger (see below).

For small values of co-operative shear the evolution remains similar to that in the first regime, but as the magnitude of the co-operative shear increases, the evolution becomes quite different. As Λ approaches $\Lambda_C \approx -1.1639$, the maximum growth rate decreases, and according to linear theory the strip should stabilize. This does not happen, as can be seen from figure 13 for $\Lambda = -1.2$. A clear sign here of a nonlinear instability mechanism is the local reduction in disturbance lengthscale before the pinching off takes place. So, although co-operative shear can suppress linear instabilities it cannot prevent nonlinear disruption.

As discussed previously (Dritschel 1989*a*, *b*), the adverse shear imposed on filaments by coherent vortices of like-signed vorticity is a major factor in the quasi-passive nature and lack of roll-up of filaments in the 2VD model. The stability results from the previous sections suggest that filaments in other two-dimensional flows (with different Green functions) should also generally behave quasi-passively. However, it is a crucial fact that the magnitude of the stabilizing shear vorticity increases as the interaction range decreases, so indeed there is likely to be more roll-up of filaments for Green functions with short interaction ranges. To demonstrate this, we consider the process of vortex merger. We are motivated in this choice by

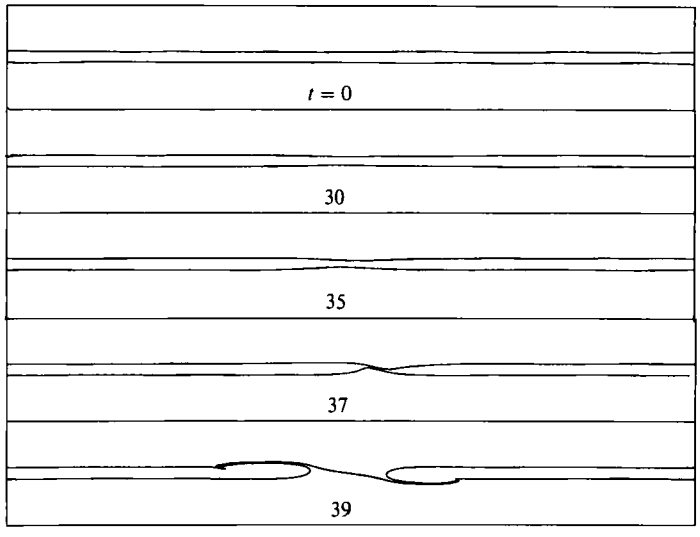

FIGURE 13. As in figure 11, but for a strip in the QGSW model ($\gamma\Delta = 1$) with co-operative shear $\Lambda = -1.2$. The strip is initially perturbed by a six-fold random disturbance with maximum amplitude 0.05Δ.

the fact that vortex merger is fundamental to the behaviour of geophysical flows. It is here that filaments are likely to be produced and then stabilized or not by the differential flow about the merged vortices. A series of calculations of the merger of two identical circular vortices with uniform PV were performed for several different Green functions. Figure 14 shows the final configurations obtained. In all cases the centroids of the vortices were initially two and a half radii apart, and the radius of deformation of the Green function is equal to the radii of the vortices. In the 2VD model, there is no sign of roll-up of the filaments shed during the coalescence of the vortices (figure 14*a*). For other models, though, as the interaction range decreases (e.g. p increases in the Green function (28)), the central vortex no longer produces enough shear to stabilize the filaments and the ends roll-up into small vortices (figure 14*b–h*). This has also been observed in the QGSW and two-layer models by Polvani, Zabusky & Flierl (1989).

8. Conclusions

In any two-dimensional model with a Green function for which the velocity on the edges of a strip of PV is finite, it has been shown that all linear instabilities can be prevented by imposing shear which reverses the shear across the strip. If additionally the Green function has a sufficiently short interaction range, the strip can also be stabilized (linearly) by imposing shear which acts in the same direction as the shear due to the strip. For thin strips of PV these stability results are essentially independent of any curvature effects. Both the linear growth rate of the disturbances and the magnitude of the shear necessary to stabilize the strip, however, are very sensitive to the interaction range of the Green function. Nonlinear calculations have shown that there will be no disruption of the strip for significantly less adverse shear than predicted by linear theory, even more so the shorter the interaction range. On the other hand, the calculations have shown that co-operative shear is not effective in preventing nonlinear disruption.

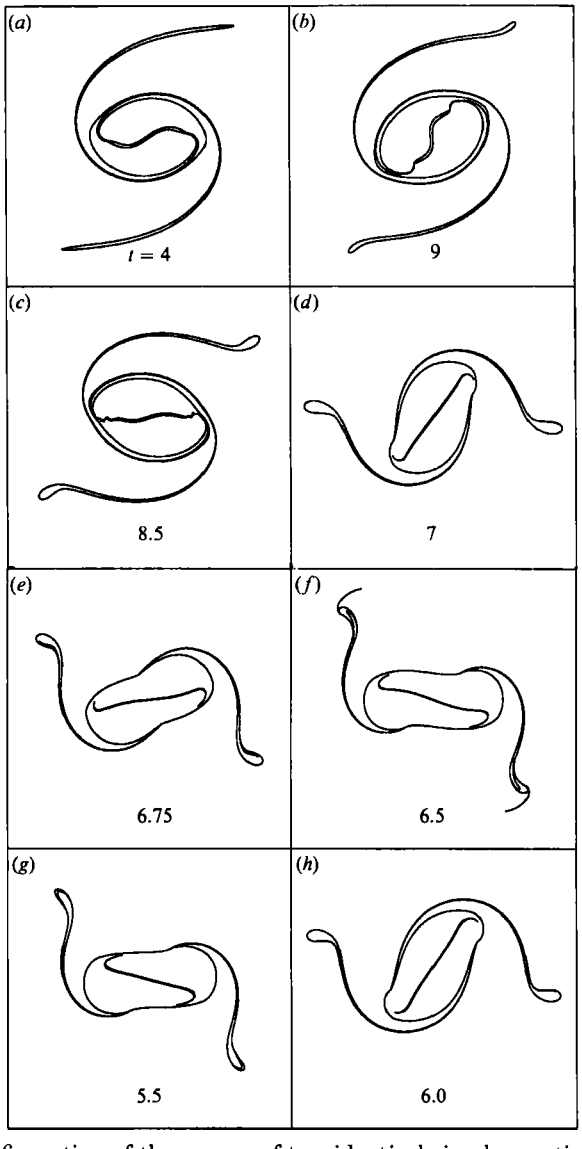

FIGURE 14. Final configuration of the merger of two identical circular vortices initially two and a half radii apart. Each vortex has potential vorticity 2π and the time is shown on each plot. (*a*) 2VD model, (*b*) hybrid Green function (28) with $p = 0.25$, (*c*) $p = 0.5$, (*d*) $p = 1.0$, (*e*) $p = 1.5$, (*f*) $p = 2.0$, (*g*) QGSW model, and (*h*) two-layer model with $\delta = 0.2$.

Polvani *et al.* (1989) and Waugh (1991) have observed that there is a suppression of filamentation in the QGSW model when the radii of the vortices are greater than a few times the radius of deformation (see also Dritschel 1989*a*, §6). This together with the above result that filaments have an increased propensity to roll-up into small vortices as the interaction range decreases, gives insight into the variation of two-dimensional flows with the PV inversion operator of the model. As stated in the Introduction, filaments are a common feature of 2VD flows and they are seldom observed to roll-up into small vortices. The above results suggest, however, that vortex interactions in models with a shorter interaction range will generate fewer filaments, and those filaments produced will tend to roll up into vortices. Hence

quasi-passive filament dynamics is not likely to typify models with short interaction ranges.

Computations were performed on the Cray X-MP at the University of London Computing Centre with the support of the Natural Environmental Research Council's UK Universities' Global Atmospheric Modelling Program. D.W.W. was supported by an Association of Commonwealth Universities Scholarship. We wish to thank P. H. Haynes for a careful reading of the manuscript.

Appendix A. Condition for stabilizing co-operative shear

As the integrals $\mathscr{I}_1(k)$ and $\mathscr{I}_2(k)$ given by (5) take their maximum value in the limit $k \to 0$, the stabilizing co-operative shear (10*b*) is

$$\Lambda_C = 1 - \frac{1}{\mathscr{I}_0(\Delta)} \lim_{k\to 0} \{\mathscr{I}_1(k) + \mathscr{I}_2(k, \Delta)\}.$$

For Λ_C to exist $\lim_{k\to 0} \mathscr{I}_1(k) = 2 \lim_{k\to 0} \int_0^\infty G(x) \cos kx \, dx$

$$= 2\int_0^\delta G(x)\,dx + 2\lim_{k\to 0}\int_\delta^\infty G(x)\cos kx\,dx \qquad (A\ 1)$$

must be finite. The first integral exists if $G(r)$ is less singular than $1/r$ at $r = 0$, since $\int_0^\delta x^{-p}\,dx$ is defined only for $p < 1$. Assuming that $G(r) \propto r^{-q}$ $(q > 0)$ for large r, and that δ is such that $k\delta < 1$, we may write the second integral as

$$2\lim_{k\to 0}\int_0^\infty x^{-q}\cos kx\,dx = 2\int_\delta^\infty x^{-q}\,dx + 2\lim_{k\to 0}\int_\delta^\infty [-\tfrac{1}{2}k^2x^{2-q} + O(k^4x^{4-q})\cos kx]\,dx.$$

The right-hand side of this expression exists only if $q > 1$, and then the second term vanishes.

Hence (A 1) is finite if $G(r)$ is less singular than $1/r$ as $r \to 0$ and decays faster than $1/r$ as $r \to \infty$, and then

$$\lim_{k\to 0} \mathscr{I}_1(k) = 2\int_0^\infty G(x)\,dx.$$

Similarly it can be shown that $\lim_{k\to 0} \mathscr{I}_2(k, \Delta)$ exists for $G(r)$ satisfying these conditions. We may then write the stabilizing co-operative shear as

$$\Lambda_C = \frac{2\mathscr{I}_2(0, \Delta)}{\mathscr{I}_2(0, \Delta) - \mathscr{I}_1(0)} < 0.$$

Note that since $G(x) - G((x^2 + \Delta^2)^{\frac{1}{2}})$ vanishes as $x \to \infty$, the integral $\mathscr{I}_0$ given by (5*a*) will exist if $\int_0^\delta G(x)\,dx$ exists. As stated above, this implies that $G(r)$ must be less singular than $1/r$ as $r \to 0$.

Appendix B. Background potential vorticity δq and point-vortex strength $\delta\Gamma$

In this Appendix we calculate the uniform background potential vorticity δq and the increment point-vortex strength $\delta\Gamma$, so that the shear at the edges of a circular strip of PV is comparable with that in the straight case, i.e. so that the constraints

(17) are satisfied. The total angular velocity due the circular strip, uniform background PV, and central point vortex is $\Omega = \Omega_s + \Omega_b + \Omega_v$, where

$$\Omega_s(r) = q(\mathscr{F}(a,r) - \mathscr{F}(b,r)) \equiv q\alpha_s(r),$$
$$\Omega_b(r) = -\delta q \mathscr{F}(R,r) \equiv \delta q \alpha_b(r)$$

(here R is some radius much larger than any other lengthscale in the flow) and

$$\Omega_v(r) = (\Gamma + \delta\Gamma)\, G'(r)/r \equiv (\Gamma + \delta\Gamma)\, \alpha_v(r).$$

The values of δq and $\delta\Gamma$ are then determined to satisfy (17a, b). Defining $\beta_s^{\pm} = \alpha_s(b) \pm \alpha_s(a)$, etc., the result is

$$\delta q = -q[\beta_s^- - \beta_s^+ \beta_v^-/\beta_v^+ - 2\hat{\Omega}]/[\beta_b^- - \beta_b^+ \beta_v^-/\beta_v^+],$$

and

$$\delta\Gamma = -\Gamma - (q\beta_s^+ + \delta q\, \beta_b^+)/\beta_v^+.$$

Appendix C. Dispersion relation for a thin circular strip of potential vorticity

The form of the dispersion relation (19), for a circular strip of uniform potential vorticity, in the limit of a thin strip ($\Delta = b - a \ll a$) is now determined. In this limit the integral $\mathscr{K}_m(a,b)$ (cf. (16)) may be written as

$$\mathscr{K}_m(a,b) = m \int_{-\pi}^{\pi} G([\Delta^2 + 2a^2(1-\cos\phi)]^{\frac{1}{2}}) \cos m\phi \, \mathrm{d}\phi.$$

For the Green functions under consideration, the significant contribution to this integral comes from small ϕ, roughly $\phi < \Delta/a$. Therefore we may use $2(1-\cos\phi) \approx \phi^2$, so

$$\mathscr{K}_m(a,b) \doteq k \int_{-a\pi}^{a\pi} G((\Delta^2 + x^2)^{\frac{1}{2}}) \cos kx \, \mathrm{d}x,$$

where we have let $x = a\phi$ and $k = m/a$. In the limit of a thin strip, $a \to \infty$ for fixed Δ, and so the integration is from $-\infty$ to ∞, and the above integral is the same as (5c), i.e.

$$\mathscr{K}_m(a,b) = k\mathscr{I}_2(k,\Delta)$$

in the limit of a thin circular strip. Similarly it can be shown that $\mathscr{K}_m(b,a) = k\mathscr{I}_2(k, \Delta)$ and $\mathscr{K}_m(a,a) = \mathscr{K}_m(b,b) = k\mathscr{I}_1(k)$, and $m\hat{\Omega} = -k\mathscr{I}_0(1-\Delta)$. Thus (19) reduces to

$$\hat{\sigma} = \pm k\{[\mathscr{I}_1 - \mathscr{I}_0(1-\Delta)]^2 - \mathscr{I}_2^2\}^{\frac{1}{2}},$$

and this is exactly the same dispersion relation as for a straight strip, equation (7).

Appendix D. Integrals for QGSW model

In this Appendix we calculate various integrals used in §2, for the QGSW model. In all cases the integrals reduce to those for 2VD when $\gamma \to 0$. The integrals (5), used in the analysis for a straight strip of uniform vorticity, are

$$\mathscr{I}_0 = -\frac{1}{2\gamma}(1 - \mathrm{e}^{-\gamma\Delta}),$$

$$\mathscr{I}_1 = -\frac{1}{2(k^2+\gamma^2)^{\frac{1}{2}}},$$

and
$$\mathscr{I}_2 = -\frac{1}{2(k^2+\gamma^2)^{\frac{1}{2}}} e^{-A(k^2+\gamma^2)^{\frac{1}{2}}},$$

while the integrals used in (18) are

$$\mathscr{K}_m(r_j, r_k) = \begin{cases} -m\left(\frac{r_j}{r_k}\right) K_m(\gamma r_k) I_m(\gamma r_j), & r_j < r_k, \\ -m\left(\frac{r_j}{r_k}\right) K_m(\gamma r_j) I_m(\gamma r_k), & r_j > r_k, \end{cases}$$

where I_m and K_m are the modified Bessel functions of the mth order. The functions of r used in Appendix C to calculate the angular velocity due to a circular strip of potential vorticity, background potential vorticity, and a point vortex are

$$\alpha_s(r) = \begin{cases} -[aI_1(\gamma a) - bI_1(\gamma b)] K_1(\gamma r)/r, & r > b, \\ -aI_1(\gamma a) K_1(\gamma r)/r + bI_1(\gamma r) K_1(\gamma b)/r, & a < r < b, \\ -[aK_1(\gamma a) - bK_1(\gamma b)] I_1(\gamma r)/r & r < a, \end{cases}$$

$$\alpha_b(r) = RK_1(\gamma R) I_1(\gamma r)/r,$$

and
$$\alpha_v(r) = \frac{\gamma}{2\pi} K_1(\gamma r)/r.$$

REFERENCES

ARNOL'D, V. I. 1965 Conditions for non-linear stability of stationary plane curvilinear flows of an ideal fluid. *Dokl. Akad. SSSR* **162**, 975–978. (Transl. in *Sov. Maths.* **6** (1965), 773–777.)

ARNOL'D, V. I. 1966 On an a priori estimate on the theory of hydrodynamic stability. *Izv. Vyssh. Uchcbn. Zaved. Matematika* **54**, 3–5. (Transl. in *Am. Math. Trans. Series 2* **79** (1969), 267–269.)

BENZI, R., PATARNELLO, S. & SANTANGELO, P. 1987 On the statistical properties of two-dimensional turbulence. *Europhys. Lett.* **3**, 811–818.

BENZI, R., PIERINI, S., VULPIANI, A. & SALUSTI, E. 1982 On the hydrodynamic stability of planetary vortices. *Geophys. Astrophys. Fluid Dyn.* **20**, 293–306.

COUDER, Y. & BASDEVANT, C. 1986 Experimental and numerical study of vortex couples in two-dimensional flows. *J. Fluid Mech.* **173**, 225–251.

DHANAK, M. R. 1981 The stability of an expanding circular vortex layer. *Proc. R. Soc. Lond.* A **375**, 443–451.

DRITSCHEL, D. G. 1986 The nonlinear evolution of rotating configurations of uniform vorticity. *J. Fluid Mech.* **172**, 157–182.

DRITSCHEL, D. G. 1988 The repeated filamentation of two-dimensional vorticity interfaces. *J. Fluid Mech.* **194**, 511–547.

DRITSCHEL, D. G. 1989*a* Contour dynamics and contour surgery: Numerical algorithms for extended, high-resolution modelling of vortex dynamics in two-dimensional, inviscid, incompressible flows. *Comput. Phys. Rep.* **10**, 77–146.

DRITSCHEL, D. G. 1989*b* On the stabilization of a two-dimensional vortex strip by adverse shear. *J. Fluid Mech.* **206**, 193–221 (referred to herein as D).

DRITSCHEL, D. G., HAYNES, P. H., JUCKES, M. N. & SHEPHERD, T. G. 1991 The stability of a two-dimensional vorticity filament under uniform strain. *J. Fluid Mech.* **230**, 647–665.

DRITSCHEL, D. G. & POLVANI, L. M. 1991 The roll-up of vorticity strips on the sphere. *J. Fluid Mech.* (submitted).

GRIFFITHS, R. W. & HOPFINGER, E. J. 1987 Coalescing of geostrophic vortices. *J. Fluid Mech.* **178**, 73–97.

HEDSTROM, K. & ARMI, L. 1988 An experimental study of homogeneous lenses in a stratified rotating fluid. *J. Fluid Mech.* **191**, 535–556.

HOSKINS, B. J., MCINTYRE, M. E. & ROBERTSON, A. W. 1985 On the use and significance of isentropic potential vorticity maps. *Q. J. R. Met. Soc.* **111**, 877–946. (Also **113**, 402–404.)

JUCKES, M. N. & MCINTYRE, M. E. 1987 A high-resolution one-layer model of breaking planetary waves in the stratosphere. *Nature* **328**, 590–596.

KURGANSKIY, M. V. & TATARSKAYA, M. S. 1987 The potential vorticity concept in meteorology: a review. *Izv. Akad. Nauk SSSR FAO*). Also Corrigendum in **25**, 1346. (Transl. in *Atmos. Ocean Phys.* **23**, 587–606.)

LEGRAS, B., SANTANGELO, P. & BENZI, R. 1988 High resolution numerical experiments for two-dimensional turbulence. *Europhys. Lett.* **5**, 37–42.

MCINTYRE, M. E. & NORTON, W. A. 1991 Potential-vorticity inversion on a hemisphere. *J. Atmos. Sci.* (to appear).

MCINTYRE, M. E. & SHEPHERD, T. G. 1987 An exact local conservation theorem for finite-amplitude disturbances to non-parallel shear flows, with remarks on Hamiltonian structure and Arnol'd's stability theorems. *J. Fluid Mech.* **181**, 527–565.

MELANDER, M. V., MCWILLIAMS, J. C. & ZABUSKY, N. J. 1987 Axisymmetrization and vorticity gradient intensification of an isolated two-dimensional vortex through filamentation. *J. Fluid Mech.* **178**, 137–159.

MELANDER, M. V., ZABUSKY, N. J. & MCWILLIAMS, J. C. 1988 Symmetric vortex merger in two dimensions: causes and conditions. *J. Fluid Mech.* **195**, 303–340.

PHILLIPS, N. A. 1954 Energy transformations and meridional circulations associated with simple baroclinic waves in a two-level, quasigeostrophic model. *Tellus* **6**, 273–286.

POLVANI, L. M., ZABUSKY, N. J. & FLIERL, G. R. 1989 Two-layer geostrophic vortex dynamics. Part 1. Upper layer V-states and merger. *J. Fluid Mech.* **205**, 215–242.

RAYLEIGH, LORD 1894 *The Theory of Sound*, 2nd edn. Macmillan (also 3rd edn. 1945 Dover).

WAUGH, D. W. 1991 The efficiency of symmetric vortex merger. *J. Fluid Mech.* (submitted).

ZAKHAROV, S. B. 1977 The stability of plane vortex sheets in an ideal fluid. *Fluid Mech. Sov. Res.* **1**, 1–7. (Engl. transl. of *Uchenyye zapiski TsAGI VII* **3** (1976), 26–31.)